Supplementary Information

Magnetic Ions in Wide Band Gap Semiconductor Nanocrystals for Optimized Thermoelectric Property

Chong Xiao[a], Kun Li[a], Jiajia Zhang[b], Wei Tong[c], Zhou Li[a], Youwen Liu[a], Pengcheng Huang[a], Bicai Pan[b], Haibin Su[d], Yi Xie,[a]*

[a]*Hefei National Laboratory for Physical Sciences at the Microscale, and Collaborative Innovation Center of Chemistry for Energy Materials, University of Science & Technology of China, Hefei, Anhui, 230026, P.R. China.*
[b]*Department of Physics, University of Science & Technology of China, Hefei, Anhui, 230026, P.R. China.*
[c]*High Magnetic Field Laboratory, Chinese Academy of Sciences, Hefei, Anhui, 230031, P.R. China.*
[d]*Division of Materials Science, Nanyang Technological University, 50 Nanyang Avenue, 639798, Singapore.*

Correspondence to: yxie@ustc.edu.cn

1. Experimental Section

Synthesis. All chemicals were of analytic grade purity obtained from Sinopharm Chemical Reagent Co., Ltd and used as received without further purification. Briefly, 0.07 g of sulfur powders was dissolved into 20ml octadecylamine at 80 ^{o}C. Then, 0.262 g of copper acetylacetonate, 0.132 g of zinc acetylacetonate, and 0.177 mL dibutyltin bis(2,4-pentanedionate) were added into the S-precursor solution. After the complex solution stirred at 120 ^{o}C for 30 minutes under N_2 atmosphere, the temperature was slightly heating up to 230 ^{o}C. The mixture was maintained at 230 ^{o}C for 1.5 h under stirred, and then the reaction was quickly stopped. The nanoplates were separated from the resulting solution by centrifuge and washed for several times with ethanol and cyclohexane. For the Ni-doped Cu_2ZnSnS_4 nanocrystals, the nickel acetylacetonate as the nickel source was added into the S-precursor solution together with zinc source. For the magnetic ions fully substituted quaternary Cu_2XSnS_4 (X=Mn, Fe, Co) nanocrystals, the manganese (II) acetylacetonate, or iron (II) acetylacetonate, or cobalt (II) acetylacetonate was respectively used to replace zinc acetylacetonate while other conditions keep the same. All the samples were dried in a vacuum at 60 ^{o}C for 6 h.

Characterization: The structure of these obtained samples was characterized with the X-ray diffraction (XRD) pattern, which was recorded on a Rigaku Dmax diffraction system using a Cu Kα source (λ=1.54187 Å). X-ray photoelectron spectroscopy (XPS) measurements were performed on a VGESCALAB MK II X-ray photoelectron spectrometer with an excitation source of Mg Kα=1253.6 eV. The field emission scanning electron microscopy (FE-SEM) images were taken on a JEOL JSM-6700F SEM. High-resolution transmission electron microscopy (HRTEM) images were performed on JEOL-2010 transmission electron microscope at 200kV. Raman spectra were recorded with a LABRAM-HR Confocal Laser MicroRaman Spectrometer 750 K with a laser power of 0.5 mW. The magnetic measurement was carried out with a superconducting quantum interference device magnetometer (Quantum Design MPMS XL-7). The temperature-dependent EPR measurement of the powder sample was performed using a Bruker EMX plus model spectrometer operating at X-band frequencies (9.4 GHz) at different temperatures.

Thermoelectric properties: The organic surfactants were removed via the procedure of previously reports before fabrication of bulk samples for thermoelectric measurement.[1] Briefly, as-prepared silver chalcogenides were dispersed in cyclohexane with hydrazine solution (85% v/v) and stirring vigorously until all the nanocrystals are precipitated. The supernatant is decanted and the precipitate is washed with ethanol three for times to remove hydrazine and collected by centrifugation, and then dried in vacuum at 65 ^{o}C. After the hydrazine treatment, hot-pressed

rectangular shape samples, which obtained under 60 MPa at 400 ^{o}C for 30 min, with typical sizes of 10 mm × 4 mm × 1.5 mm were employed to simultaneously measure Electrical conductivity σ and Seebeck coefficient S by the standard four-probe methods in a He atmosphere (ULVAC-RIKO ZEM-3). Thermal conductivity κ was calculated using the equation $\kappa=a\rho C_p$ from the thermal diffusivity a obtained by a flash diffusivity method (LFA 457, Netzsch) on a hot-pressed round disc sample with diameter of about 13 mm and thickness of 2 mm (obtained under 60 MPa at 400 ^{o}C for 30 min), specific heat C_p determined by a differential scanning calorimeter method (DSC Q2000, Netzsch).

Calculation details: All calculations were handled by performing density functional theory as implemented in the Vienna ab initio Simulation Package (VASP).[2] In our calculations, the hybrid functional Heyd-Scuseria-Ernzerhof (HSE06)[3] was employed, in which the mixing parameter of 0.25 was selected. The single-particle equations were solved using the projector-augmented wave (PAW)[4] method with a plane-wave cutoff of 600 eV. A k-points mesh of 1×1×2 was used to sample the Brillouin zone of the supercell. For the electronic self-consistency loop a total energy convergence criterion of 1×10^{-4}eV was required. Lattice constants and internal coordinates were fully optimized until residual Hellmann-Feynman forces were smaller than 0.01 eV/Å.

1. *XPS Characterization of the pure and Ni-doped Cu_2ZnSnS_4 nanocrystals.*

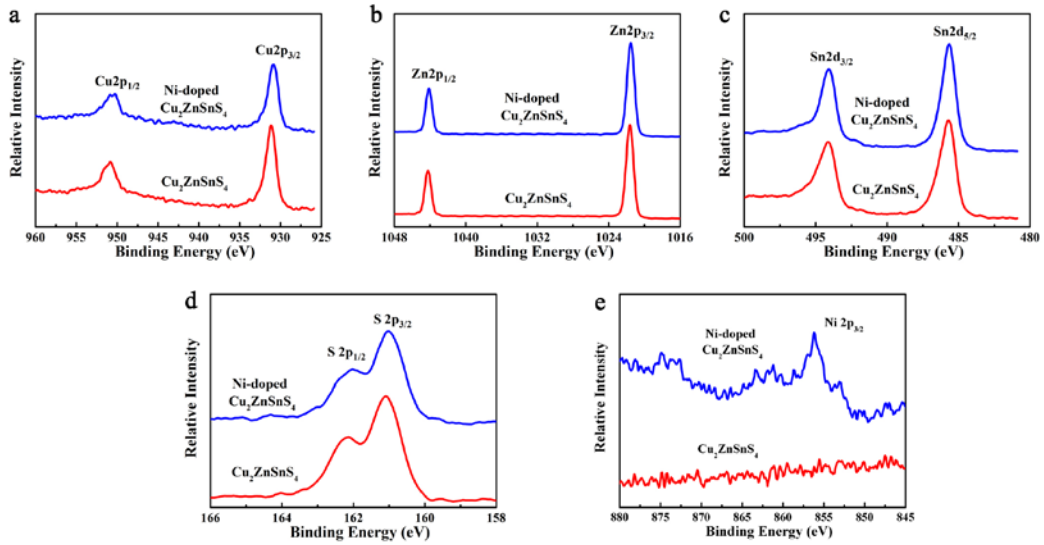

Figure S1. Core-level XPS spectra for the pure and Ni-doped Cu_2ZnSnS_4 nanocrystals.

2. *HRTEM images and SAED patterns for Ni-doped Cu_2ZnSnS_4 nanocrystals.*

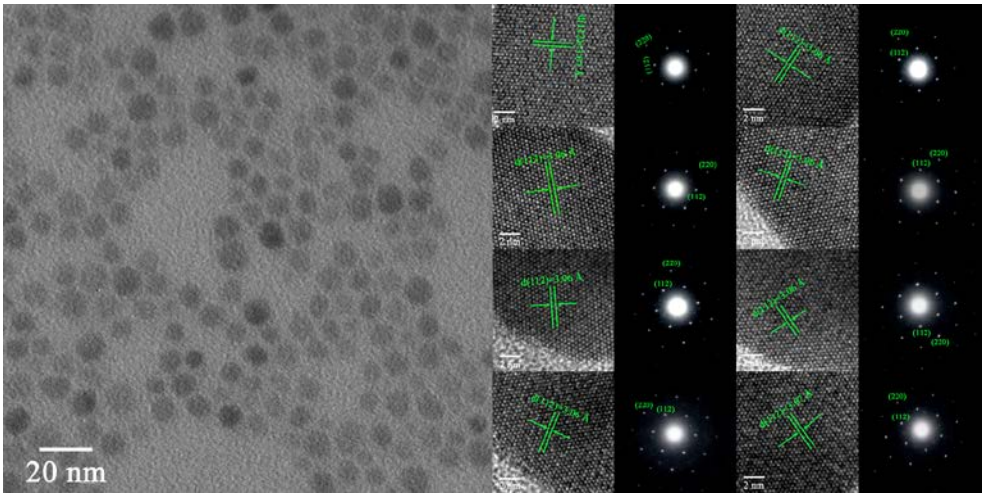

Figure S2. TEM, HRTEM and SAED patterns for the Ni-doped Cu_2ZnSnS_4 nanocrystals. The HRTEM and SAED patterns were stochastically selected from some nanoparticles.

3. *Band structure calculation for pure Cu_2ZnSnS_4.*

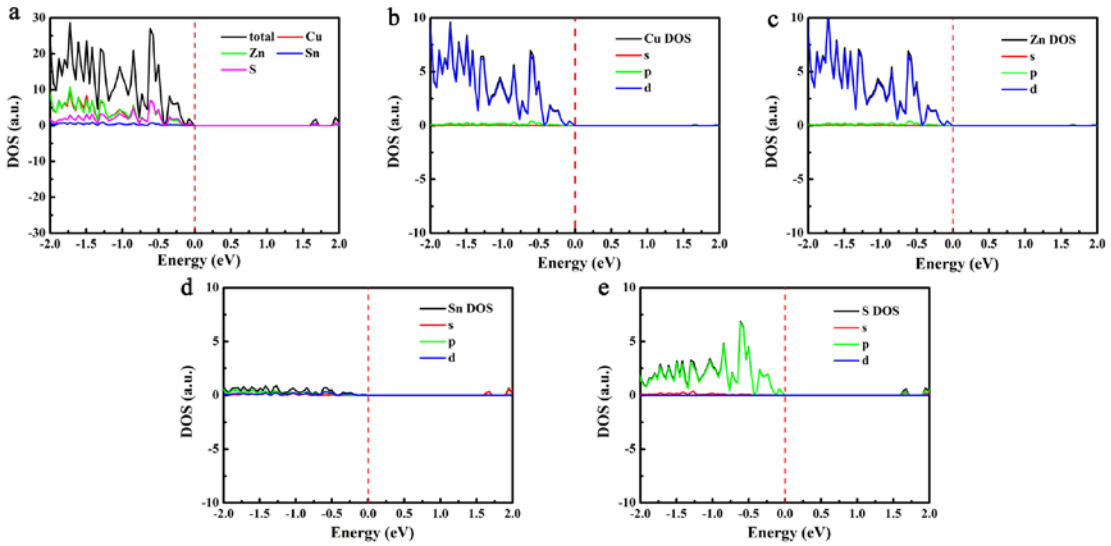

Figure S3. Density of states for pure Cu_2ZnSnS_4 nanocrystals. (a) Total density of states and atomic contributions. Partial atomic densities of states with angular momentum decomposition for Cu **(b)**, Zn **(c)**, Sn **(d)**, and S **(e)**, respectively. In the pure Cu_2ZnSnS_4, the valence band (VB) is mainly made up of the antibonding component of the hybridization between Cu/Zn 3*d* states and S 3*p* states, while an antibonding state hybrided by Sn 5*s* states and S 3*p* states makes up the conduction band (CB).

4. *Band structure calculation for Ni-doped Cu_2ZnSnS_4.*

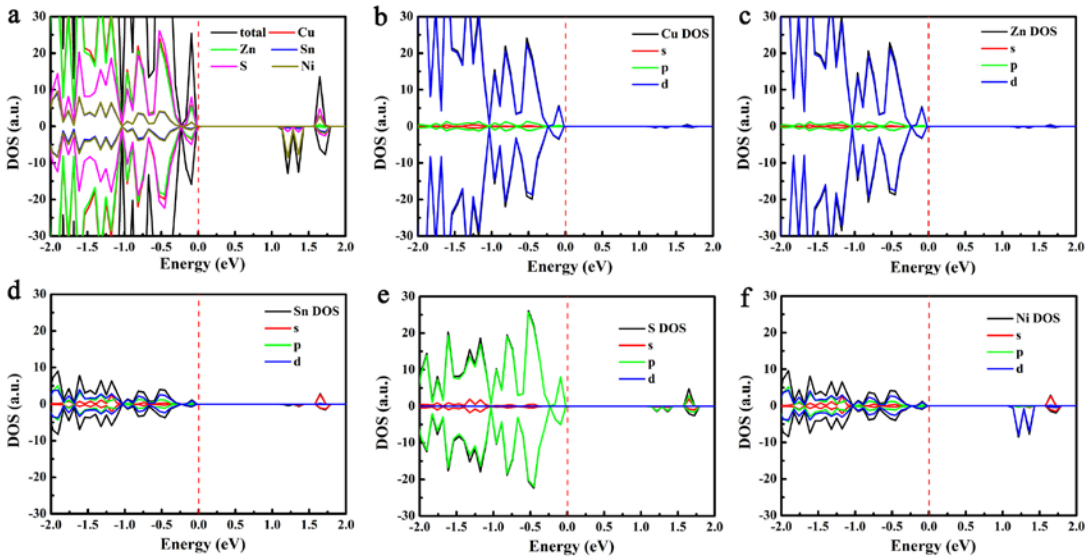

Figure S4. Density of states for Ni-doped Cu_2ZnSnS_4 nanocrystals. (a) Total density of states and atomic contributions. Partial atomic densities of states with angular momentum decomposition for Cu **(b)**, Zn **(c)**, Sn **(d)**, S **(e)**, and Ni **(f)** respectively.

5. *XPS Characterization of the Cu_2XSnS_4 (X=Mn, Fe, Co) nanocrystals.*

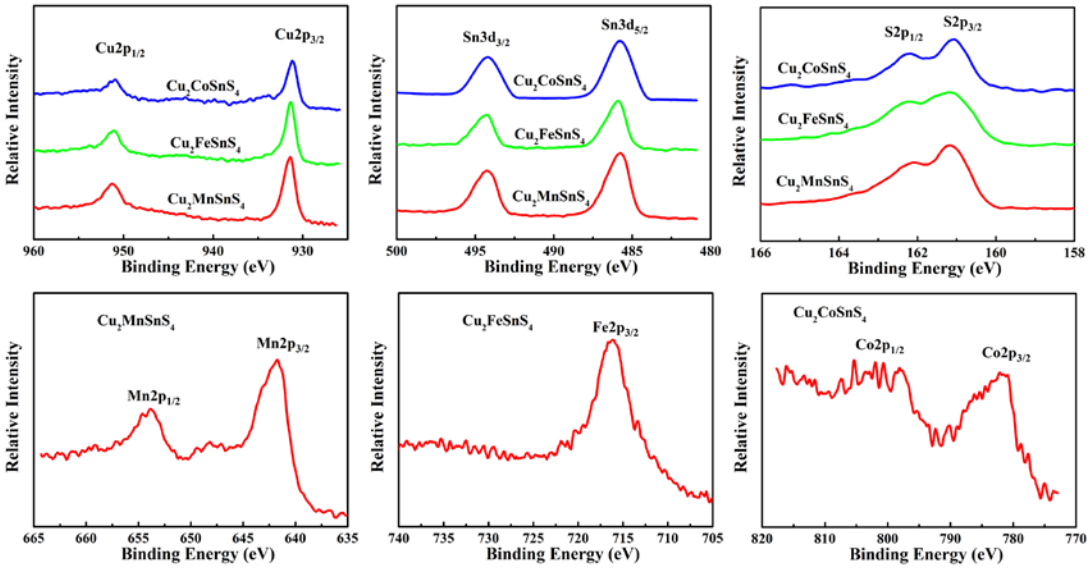

Figure S5. Core-level XPS spectra for the Cu_2XSnS_4 (X=Mn, Fe, Co) nanocrystals.

6. *Electronic and lattice thermal conductivity of the Cu_2XSnS_4 (X=Mn, Fe, Co) nanocrystals.*

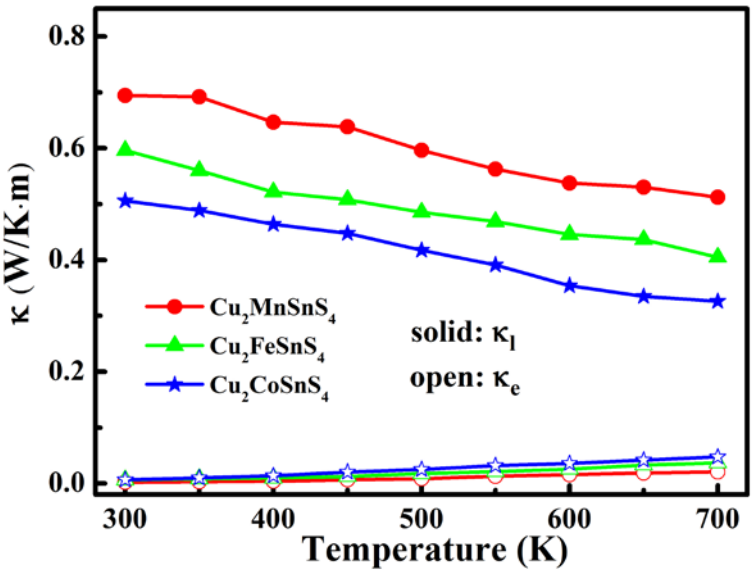

Figure S6. The calculated electronic and lattice thermal conductivity for the Cu_2XSnS_4 (X=Mn, Fe, Co) nanocrystals**.**

References

1. M. Scheele, N. Oeschler, K. Meier, A. Kornowski, C. Klinke, H. Weller, *Adv. Funct. Mater.* 2009, **19**, 3476.
2. G. Kresse, J. Furthmuller, *Phys. Rev. B* 1996, **54**, 11169.
3. J. Heyd, G. E. Scuseria, M. Ernzerhof, *J. Chem. Phys.* 2003, **118**, 8207.
4. G. Kresse, D. Joubert, *Phys. Rev. B* 1999, **59**, R1758.